doi.org/10.36721/PJPS.2026.39.10.298.1

Mechanism of astragaloside-loaded lactosyl chitosan nanoparticles inhibiting MAPK/ERK pathway and preventing angiogenesis and colon cancer development through miR-200

Renhao Chen and Bin Wang*
Department of Gastroenterology, Tongling People's Hospital, Affiliated Hospital of Wannan Medical College, Tongling, Anhui, 244000, China

Abstract: **Background**: The incidence of colorectal cancer in China continues to rise. Astragaloside IV has been shown to delay its progression and nanoparticles constructed from it with astragaloside-lactosyl chitosan nanoparticles (ALCNPs) exhibit enhanced therapeutic efficacy. **Objectives**: This study aimed to construct novel lactosyl chitosan nanoparticles (ALCNPs) to improve the delivery of astragaloside IV and to investigate its mechanism in inhibiting CRC angiogenesis and progression via the miR-200/MAPK/ERK axis. **Methods**: ALCNPs were prepared using a CRC mouse model and SW480 cells. Evaluations were conducted on proliferation, VEGF expression, MAPK and ERK protein expression, while apoptosis, invasion and MVD count were analyzed to assess angiogenesis. **Results**: ALCNPs were successfully prepared, exhibiting spherical morphology with uniform dispersion. They exerted anti-tumor effects by inhibiting angiogenesis and inducing apoptosis in CRC cells through the activation of miR-200. The underlying mechanism involves the downregulation of the MAPK/ERK signaling pathway by miR-200. **Conclusion**: ALCNPs, as an effective targeted delivery system for Astragaloside IV, can inhibit the MAPK/ERK signaling pathway by upregulating miR-200, thereby suppressing angiogenesis, inducing tumor cell apoptosis and slowing CRC progression.

Keywords: ALCNPs; Angiogenesis; Colon cancer; miR-200; MAPK/ERK pathway

Submitted on 20-03-2025 – Revised on 31-12-2026 – Accepted on 25-03-2026

INTRODUCTION

Colorectal cancer (CRC) is a malignant tumor that poses a serious threat to human health worldwide. According to epidemiological statistics, there were over 1.9 million new CRC cases and approximately 935,000 deaths globally in 2020 (Xi and Xu, 2020). Among these, the burden of incidence and mortality in China continues to rise, making CRC one of the top five cancer types in terms of incidence in the country (Qiu *et al*., 2025). Compared to Western countries, the onset of CRC in China shows a trend toward younger age, with a lower rate of early diagnosis. Most patients are diagnosed at an advanced stage, leading to increased treatment challenges and poor prognosis (Maomao *et al*., 2022). Therefore, gaining an in-depth understanding of the molecular mechanisms underlying the occurrence and development of CRC and exploring more effective and less toxic novel treatment strategies hold significant clinical and social value.

The progression of CRC is a complex, multi-stage process involving multiple factors, among which tumor angiogenesis is a key mechanism supporting rapid tumor growth and distant metastasis. Tumor cells and their microenvironment can secrete critical factors such as vascular endothelial growth factor (VEGF) and stromal cell-derived factor-1α (SDF-1α) (Yang *et al*., 2022), which induce the proliferation and migration of host vascular endothelial cells and promote the formation of new vascular networks, thereby supplying the tumor with essential oxygen and nutrients (Zhang *et al*., 2021). Inhibiting angiogenesis has become a significant direction in targeted therapy for CRC. However, existing anti-angiogenic drugs face challenges such as drug resistance, making it imperative to explore novel regulatory targets and combined intervention strategies.

At the molecular regulation level, the miR-200 family, as important post-transcriptional regulators, plays a key role in maintaining epithelial cell phenotypes, inhibiting epithelial-mesenchymal transition (EMT) and regulating tumor metastasis (Gorecki and Rak, 2021). Studies have shown that miR-200 is often downregulated in various solid tumors, including CRC and its expression level is significantly associated with tumor invasiveness and poor patient prognosis (Cınar Ayan *et al*., 2021). Recent research indicates that miR-200 can not only directly target oncogenes but also indirectly influence tumor progression by regulating signal communication among stromal cells within the tumor microenvironment (Chen *et al*., 2022). However, whether and how miR-200 affects CRC angiogenesis by regulating downstream signaling pathways has not been fully elucidated.

Among the numerous signaling pathways, abnormal activation of the MAPK/ERK pathway is closely associated with the proliferation, survival, invasion and

**Corresponding author:* e-mail: yuanjifuguan@126.com

angiogenesis of CRC (Li *et al*., 2023). This pathway can be activated by various growth factors and cytokines, leading to the upregulation of pro-angiogenic factors such as VEGF (Liu *et al*., 2023). Research has shown that targeting the MAPK/ERK pathway can effectively inhibit the growth and angiogenesis of CRC (Pashirzad *et al*., 2021). Notably, recent studies suggest that members of the miR-200 family may exert negative regulation on MAPK/ERK signaling activity by targeting key nodal molecules within this pathway (Dai *et al*., 2024). This provides new insights for exploring CRC treatment from the perspective of "microRNA-signaling pathway" interactions.

In recent years, nano-targeted delivery systems based on natural active ingredients have provided new approaches for tumor therapy. Astragaloside, the main active component extracted from the traditional Chinese medicine Astragalus, has been confirmed by research to possess anti-inflammatory, antioxidant, immunomodulatory and potential anti-tumor activities, demonstrating therapeutic potential in various disease models, including CRC (Wang *et al*., 2023). However, its poor water solubility, low bioavailability and weak targeting ability limit its clinical application. Lactosylchitosan Liposome Nanoparticles (LCLNPs), as a biocompatible active targeting delivery system, can enhance drug accumulation in the liver and tumor tissues with high expression of the asialoglycoprotein receptor (ASGPR) on the surface of hepatocytes through the specific binding of lactose residues to ASGPR. This improves efficacy and reduces systemic toxicity (Zhou *et al*., 2025) and is widely used in the field of drug delivery (Yu *et al*., 2024). Therefore, this study innovatively constructed Astragaloside-loaded LCLNPs (Astragaloside-LCLNPs, ALCNPs) and aims to systematically investigate their therapeutic effects and molecular mechanisms on CRC. This study hypothesizes that ALCNPs may upregulate the low expression of miR-200 in CRC, thereby inhibiting the excessive activation of the downstream MAPK/ERK signaling pathway. Ultimately, this could synergistically suppress tumor angiogenesis, induce tumor cell apoptosis and delay the progression of CRC. The proposed mechanism of action is illustrated in fig. 1. The findings are expected to provide a new candidate drug and theoretical foundation for the targeted therapy of CRC.

MATERIALS AND METHODS

Main experimental reagents and materials

Astragaloside IV (purity 98%; Astragaloside Bolin Creatures, China); Chitosan (GS Haizhiyuan Bio); Lactosylchitosan (GC Sichuan Institute of Antibiotics); Sodium Tripolyphosphate (TPP Sinopharm Group); VEGF Antibody (Abcam); miR -200 inhibitor (Shanghai Ruibo); SB202190 (MCE, USA); fetal bovine serum (Yizefeng Biotechnology (Shanghai)); CO2 incubator (Eppendorf Eppendorf China); RNA extraction kit (Shanghai Yudao Biotechnology) ; Reverse transcription kit (GeneCopoeia, USA); CCK-8 kit (Fuyuan (Shanghai) Bio); Flow cytometry (Shanghai Yuyan).

Experimental animals and grouping

Twenty-four 4-week-old Balb/c male nude mice, with an average weight of 22±2 g, were purchased from Chengdu Dashuo Experimental Animal Company. After one week of acclimatization, the mice were housed in standard clean cages under controlled environmental conditions (temperature: 22±2°C, humidity: 60% and a 12:12-hour light-dark cycle). They were provided with unlimited feed and sterilized water. The 24 mice were randomly divided into 4 groups (n=6 per group): (1) Control group (intravenous tail injection of normal saline); (2) ALCNPs group (intravenous tail injection of ALCNPs, with an astragaloside dose of 50 mg/kg); (3) ALCNPs + interference miR-200 group (intravenous tail injection of ALCNPs at an astragaloside dose of 50 mg/kg, combined with intratumoral injection of 20 nmol/L of miR-200 inhibitor); (4) ALCNPs+interfering miR-200+SB202190 group (intravenous tail injection of ALCNPs + intratumoral injection of both miR-200 inhibitor and p38 MAPK inhibitor SB202190).

The ALCNPs + interfering miR-200 + SB202190 group was established to verify whether pharmacological inhibition of its downstream MAPK signaling (p38 MAPK) could partially restore the anti-tumor effects of ALCNPs after miR-200 function was suppressed, thereby validating the regulatory axis of "miR-200 and the MAPK pathway."

The sample size was determined based on the results of preliminary experiments and statistical power analysis from previous similar studies (Li *et al*., 2025a). The dosage of astragaloside at 50 mg/kg was established based on preliminary experiments conducted for this study and relevant literature (Rahman *et al*., 2024).

Except for the Control group, the remaining three groups received subcutaneous injections of 5×10^6 cells into the left axilla of the mice. One week later, when the tumor volume reached 90 mm^3, mice in each group were administered the corresponding drug interventions for a total of 7 sessions. Finally, all mice were sacrificed to collect tumor tissues.

Cell culture and treatment

The human colorectal cancer cell line SW480 (ATCC CCL-228™) was purchased from the American Type Culture Collection (ATCC). All cells were authenticated using STR profiling prior to use and confirmed to be mycoplasma-negative. SW480 cells were cultured in RPMI1640 medium supplemented with 10% fetal bovine serum and 1% penicillin/streptomycin. SW480 cells in logarithmic growth phase were used for nano-intervention and assigned into Control group (0 μmol/L Astragaloside-GC-NPs) and ALCNPs group (50 μmol/L Astragaloside-GC-NPs).

Preparation of ALCNPs

Add GC to 1% acetic acid aqueous solution for dissolving treatment, stir to obtain clear N-GC and dissolve it, then add an appropriate amount of drug Astragaloside to the N-GC solution to adjust the pH value. Under magnetic stirring, add 1.0 mg/mL TPP solution evenly into the solution at room temperature at a speed of 1 drop/2 s. When the color of the solution turned into a light blue emulsion, stop dripping and continue stirring for 30 minutes and filter through a 0.45 μm microporous membrane to obtain Astragaloside-GC-NPs colloidal solution.

Characterization of ALCNPs

Morphological observation

A droplet of the ALCNP solution was placed on a silicon wafer, dried at room temperature and sputter-coated with gold. The microstructure of the nanoparticles was then observed using scanning electron microscopy (SEM).

Particle size, polydispersity index (PDI) and zeta potential

The hydrodynamic particle size, PDI and zeta potential of the ALCNP colloidal solution were measured at 25℃ using dynamic light scattering (DLS). Each sample was measured three times and the results are expressed as mean ± standard deviation.

Encapsulation efficiency and drug loading capacity

An aliquot of the ALCNP solution was centrifuged at 12,000 rpm for 30 minutes at 4℃ to separate the free drug. The supernatant was collected and the content of free astragaloside was quantified using high-performance liquid chromatography (HPLC). The encapsulation efficiency (EE%) and drug loading capacity (DL%) were calculated using the following formulas: EE% = (Total drug input - Free drug amount) / Total drug input × 100%; DL% = (Total drug input - Free drug amount) / Total weight of nanoparticles × 100%. The total weight of the nanoparticles was determined by lyophilizing a known volume of the ALCNP solution and weighing the resulting solid.

Experimental method

Colony assay to detect CRC cell proliferation

After 14 days of culture, cells were fixed, stained and observed to assess the formation of colony units.

Detection of CRC cell proliferation by CCK-8

Cells (1×10^3) were placed in 96-well culture dishes. Add 10 microliters of CCK-8 reagent for 2 hours' incubation and then read the absorbance at 450 nm (Dong *et al.,* 2019).

qRT-PCR

RNA was extracted for cDNA synthesis followed by RT-qPCR. For mRNA analysis, GAPDH was used as the internal reference gene and for miRNA analysis, U6 snRNA was used as the internal reference. Real-time fluorescence quantitative PCR was performed using the SYBR Green method. The relative expression levels of the target genes were calculated using the $2^{-\Delta\Delta Ct}$ method. All experiments were conducted with three technical replicates and independently repeated three times. Table 1 lists the primers and the sequence of the primers.

Western blot

Cells were lysed and separated for western blot analysis of protein expression. Protein level was detected with a chemiluminescent detection kit.

Apoptosis analysis by flow cytometry

CRC cells were transfected and cultured for 24 hours, digested and made into 1×10^6ml cell suspension, centrifuged, washed, resuspended, added 5μl PI and 10μl Annexin V-FITC, incubated for 0.25h and analyzed by flow cytometry (Zhang *et al.,* 2022).

Transwell detection of cell invasion and migration ability

Cell migration: Cells from each group were resuspended in serum-free medium and seeded into the upper chamber of a Transwell insert (polycarbonate membrane, 8 μm pore size) at a density of 1×10^5 cells/mL. The lower chamber was filled with complete medium containing 10% fetal bovine serum or SDF-1α (100 ng/mL) as a chemoattractant. After 12 hours of incubation, the inserts were removed, rinsed with PBS, fixed with 4% paraformaldehyde and stained with 0.1% crystal violet. The number of cells that migrated through the membrane was counted under a microscope in five randomly selected fields (×200 magnification) (Lu *et al.,* 2022).

Cell invasion: Based on the migration assay, the polycarbonate membrane of the Transwell upper chamber was pre-coated with Matrigel (50 μL/chamber, diluted in serum-free medium) and polymerized at 37ºC for 2 hours to form a gel layer. Subsequent steps, including cell seeding, incubation, fixation, staining and counting, were performed identically to the migration assay. Observations were conducted using a conventional microscope and image analysis was performed.

MVD counting detection of angiogenesis (DAB staining)

Prepare vascular wax blocks, slice them, bake at 60ºC for 24 hours, wash, incubate, wash, block with goat serum for 2 hours, primary antibody (1:100), wash twice with PBS, Each time for 3 minutes, secondary antibody incubation for 2 hours, PBS washing 3 times, each time for 3 minutes, DAB chromogenic solution and 1ml DAB substrate solution were mixed, incubated, washed, hematoxylin stained nuclei, alcohol color separation, dilute ammonia water reversed blue, gradient ethanol If it is watery, make it transparent, seal the slide, place it under a microscope for observation and take pictures for records.

Table 1: Primer sequences.

Primer		Sequences
VEGF	Forward primer	5'-CGAGCTGTACAACTCCAGTG-3'
	Reverse primer	5'-GGGTAACGCCAGGAATTGTT-3'
MAPK	Forward primer	5'-TCCCTGGAGACCTGAGAACACC-3'
	Reverse primer	5'-GCTGCCATTGAACAGCGTCTC-3'
ERK	Forward primer	5'-TGAGGGGAGATGAACAACTC-3'
	Reverse primer	5'-GCCATCCGTAGTAGGTGGTG-3'
GAPDH	Forward primer	5'-AAAGGGTCATCATCTCCGCC-3'
	Reverse primer	5'-AGTGATGGCATGGACTGTGG-3'
miR-200	Forward primer	5'-GCCGTCTAACACTGTCTGGTA-3'
	Reverse primer	5'-CCTACGCCACAATTAACAAGCC-3'
U6	Forward primer	5'-CTCGCTTCGGCAGCACA-3'
	Reverse primer	5'-AACGCTTCACGAATTTGCGT-3'

Tumor tissue weight

The weight of the tumor tissue was weighed by weighing.

Statistical analysis

All quantitative experiments were independently repeated at least three times. Data are presented as mean ± standard deviation. Statistical analysis was performed using SPSS 27.0 software. Comparisons among multiple groups were conducted using one-way analysis of variance (ANOVA). For pairwise comparisons between groups, the LSD method was used when variances were homogeneous and Tamhane's T2 method was applied when variances were heterogeneous. Comparisons between two groups were performed using the independent samples t-test. A P-value < 0.05 was considered statistically significant.

RESULTS

Successful preparation of ALCNPs

Scanning electron microscopy (SEM) observation confirmed that Astragaloside-GC-NPs are spherical with a regular shape, a smooth surface and good dispersibility (Fig. 1A). Dynamic light scattering (DLS) analysis revealed that the prepared Astragaloside-GC-NPs have a hydrated particle size of 175.60 ± 26.79 nm (Fig. 1B) and a polydispersity index (PDI) of 0.152 ± 0.023 (Fig. 1C), indicating uniform particle size and a narrow distribution. The zeta potential was measured at 28.5 ± 1.2 mV (Fig. 1D). The relatively high positive charge is beneficial for the colloidal stability of the nanoparticles and may promote their binding to negatively charged cell membranes through electrostatic interactions. High-performance liquid chromatography (HPLC) analysis showed that the encapsulation efficiency of Astragaloside-GC-NPs was 82.4% ± 3.1% and the drug loading capacity was 9.7% ± 0.5%, demonstrating the high drug loading efficiency of this nano-delivery system.

Anticancer effect of ALCNPs on CRC cells

In order to explore whether Astragaloside-GC-NPs has anticancer effect on CRC cells, we detected the biological behavior of CRC cells. Astragaloside-GC-NPs could reduce proliferation ability of CRC cells (VS Control, $P<0.05$ $P<0.01$ Figs. 2A-B); the expression of apoptosis-related proteins and the apoptosis rate of CRC cells reflected that Astragaloside-GC-NPs can induce apoptosis or promote apoptotic cell death of cancer cells (VS Control, $P<0.05$ Figs. 2C-E). In addition, it is found that Astragaloside-GC-NPs can reduce the invasion and migration of cancer cells (VS Control, $P<0.05$ $P<0.01$ Figs. 2F-G).

ALCNPs induces CRC cell apoptosis by inhibiting angiogenesis

In order to further explore whether Astragaloside-GC-NPs can induce CRC cell apoptosis by inhibiting angiogenesis, we established a CRC mouse model by subcutaneously transplanting CRC cells and administered corresponding treatments via tail vein injection. Astragaloside-GC-NPs could inhibit the formation of new blood vessels (VS Control $P<0.01$ Fig. 3A) and VEGF expression in tumor tissue was also significantly reduced (VS Control $P<0.01$ Fig. 3B). Additionally, Astragaloside-GC-NPs can reduce the tumor volume (VS Control $P<0.05$ Fig. 5C); the results of apoptotic proteins showed increased expression of pro-apoptotic proteins while decreased expression of anti-apoptotic proteins (VS Control $P<0.05$ Figs. 3C-E); When detecting the apoptosis rate of tumor tissue, it was observed that Astragaloside-GC-NPs could increase the apoptosis of cells in tumor tissue (VS Control $P<0.05$ Fig. 3F), so as to achieve the therapeutic effect on CRC.

ALCNPs activates miR-200 expression, inhibits angiogenesis and induces apoptosis of CRC cells

In order to explore the specific mechanism that Astragaloside-GC-NPs can cause CRC cells to undergo apoptosis, we detected the changes in the level of miR-200 in tumor tissues. The results showed that Astragaloside-GC-NPs could increase the expression of miR-200 in tumor tissue (VS Control $P<0.05$ Fig. 4A); when interfering with miR-200, it was found that miR-200 could restore and increase the expression of VEGF in tumor

tissue and the number of new blood vessels was increased (VS Control P<0.05 Fig. 4B-C); after miR-200 interference, Caspase-3 and Bax expression was reduced and Bcl-2 was increased (Control P<0.05 Figs. 6D-E), in addition, CRC cells apoptosis also decreased significantly (Control P<0.05 Fig. 4F).

ALCNPs can inhibit the expression of MAPK/ERK

Next, we tested whether Astragaloside-GC-NPs could change the activity of MAPK/ERK signaling pathway. Western blot results indicated that, compared to the control group, ALCNP treatment significantly reduced the levels of both p-ERK and phosphorylated p-p38 MAPK in CRC cells and tumor tissues (P < 0.05, Fig. 5). When a miR-200 inhibitor was introduced, the reduction in p-ERK and p-p38 MAPK was partially reversed, suggesting that the upregulation of miR-200 is associated with the inhibition of MAPK signaling pathway activity, including both the ERK and p38 MAPK branches.

ALCNPs induces apoptosis of CRC cells by inhibiting MAPK/ERK through miR-200

To further investigate whether ALCNPs affect cell apoptosis by modulating the MAPK pathway through miR-200, we co-administered the specific p38 MAPK inhibitor SB202190 along with the miR-200 inhibitor. It was found that SB202190 can inhibit the abnormal increase of angiogenesis caused by interference with miR-200 and the number of MVD counts was significantly reduced (VS Astragaloside-GC-NPs+miR-200 inhibitor+SB202190, P<0.05 Fig. 6A) and VEGF expression also decreased (VS Astragaloside-GC-NPs+miR-200 inhibitor+SB202190, P<0.05 Fig. 6A); after co-injection, it can also affect the apoptosis of tumor tissue. The phenomenon of decreased apoptosis ability, in which Bax and Caspase-3 levels were inhibited, while level of Bcl-2 was up-regulated (VS Astragaloside-GC-NPs+miR-200 inhibitor+SB202190, P<0.05 Fig. 6B-E), the apoptosis rate was also significantly increased (VS Astragaloside-GC-NPs+miR-200 inhibitor+SB202190, P<0.05 Fig. 6F). The results indicate that combined inhibition of p38 MAPK can partially reverse the enhanced angiogenesis and attenuated apoptosis caused by miR-200 inhibition. This suggests that the p38 MAPK signaling pathway is one of the key effector pathways downstream of miR-200, mediating the anti-angiogenic and pro-apoptotic effects of ALCNPs.

DISCUSSION

CRC causes about 800,000 deaths per year, accounting for 9% of all cancer deaths in the world (Morgan *et al*., 2023). Tumor stroma plays a pivotal role in the occurrence, drug resistance and recurrence of tumors (Mortezaee, 2021). In CRC, the tumor microenvironment is mainly composed of blood vessels, fibroblasts, immune cells and other substances, among which angiogenesis is a prerequisite for tumor growth and metastasis (Zhong *et al*., 2022). Angiogenesis is maintained by a combination of promoting and inhibiting factors and when this homeostasis changes, new blood vessels are generated, thereby accelerating tumor progression (Peng *et al*., 2021). Currently, for the treatment of CRC, in addition to surgical resection, chemotherapy is an important adjuvant means (Valenzuela *et al*., 2025). However, the resistance of tumor cells to chemotherapeutic drugs is indeed an urgent clinical problem that needs to be solved.

We prepared a new type of nanoparticle (Astragaloside-GC-NPs) and studied its effect on angiogenesis and CRC development. First, dissolving Astragaloside-GC-NPs in culture medium and stimulating CRC cells revealed that Astragaloside-GC-NPs could effectively inhibit CRC cell activities and increase apoptosis ability. This suggests that Astragaloside-GC-NPs has an inhibitory effect on the growth of CRC cells, consistent with reports that Astragaloside has anti-inflammatory, immunomodulatory and anti-cancer properties (Liang *et al*., 2023; Xia *et al*., 2023). Li *et al*., (2024) found that astragaloside can increase the chemosensitivity of CRC cells to cisplatin by inhibiting NOTCH3, thereby inhibiting the development of CRC. In the study of Xu *et al*.(2023), they found that astragaloside can organize the polarization of tumor cells to M2 through the AMPK signaling pathway and then play an anti-tumor effect. The results of this study showed that Astragaloside-GC-NPs had a significant inhibitory effect on angiogenesis in CRC tumor tissue, which would not only lead to a decrease in the number of blood vessels, but also lead to a decrease in the quality of the tumor. To explore the specific role of Astragaloside-GC-NPs in inhibiting the growth of tumor cells, we detected the ability of invasion, migration and apoptosis of tumor tissues and found that Astragaloside-GC-NPs not only enhanced the rate of tumor apoptosis, but also inhibited its ability to invade and migrate, thereby inhibiting the development of CRC. Therefore, this study uses Astragaloside-GC-NPs as a therapeutic drug for CRC and explores its specific mechanism in the treatment of CRC.

miR-200 family participates in tumorigenesis (Xu *et al*., 2023). In this experiment, it was found that Astragaloside-GC-NPs can increase the expression of miR-200, consistent with the findings of Klicka *et al*. (2022) At the same time, in order to explore whether Astragaloside-GC-NPs inhibited angiogenesis and tumor growth through miR-200, we interfered with miR-200 and injected miR-200 inhibitor into mice. It was found that miR-200 inhibitor can offset the effect of Astragaloside-GC-NPs on angiogenesis and reduce the apoptosis rate of tumor tissue, which is consistent with Cheon *et al*., (2024). This suggested that Astragaloside-GC-NPs slowed the development of CRC by activating the expression of miR-200.

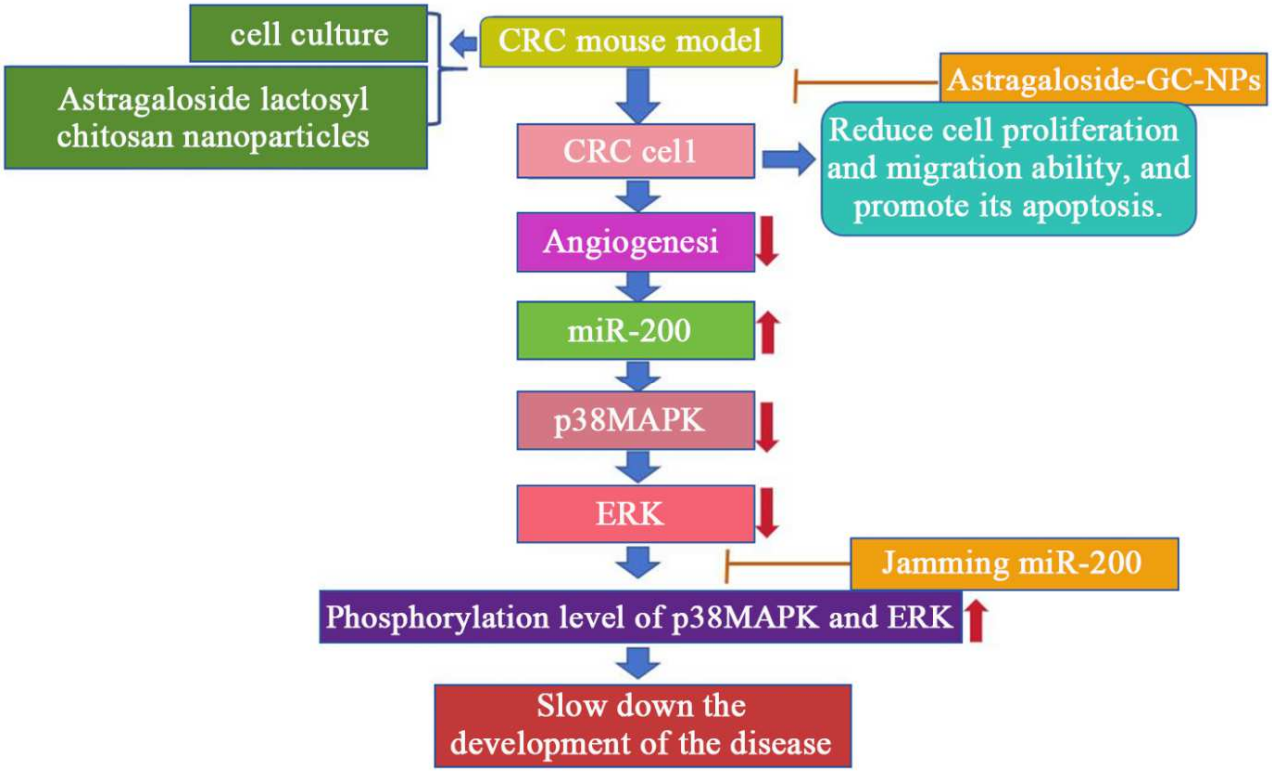

Fig. 1: Astragaloside lactosyl chitosan nanoparticles activate miR-200, inhibit MAPK/ERK pathway, hinder angiogenesis, promote tumor cell apoptosis, and slow down CRC development.

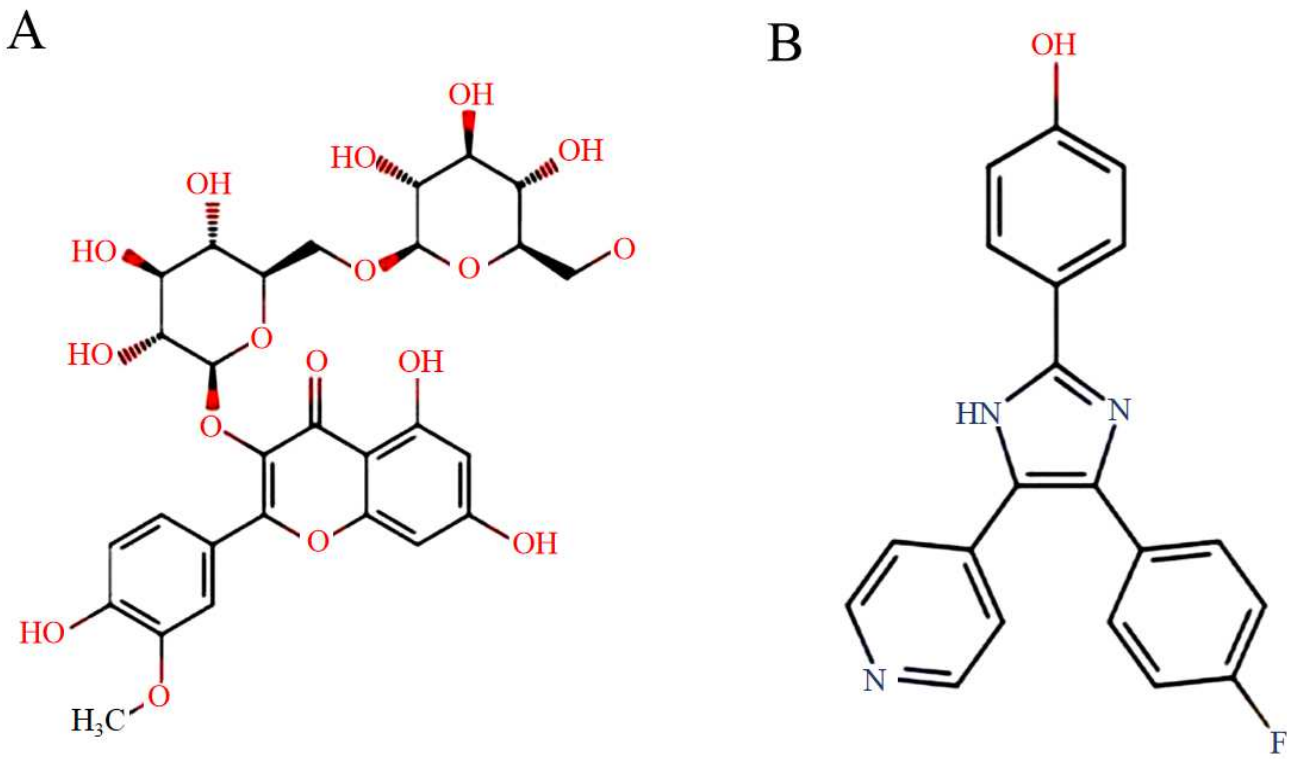

Fig. 2: Chemical molecular structure diagram of astragaloside and MAPK inhibitor.

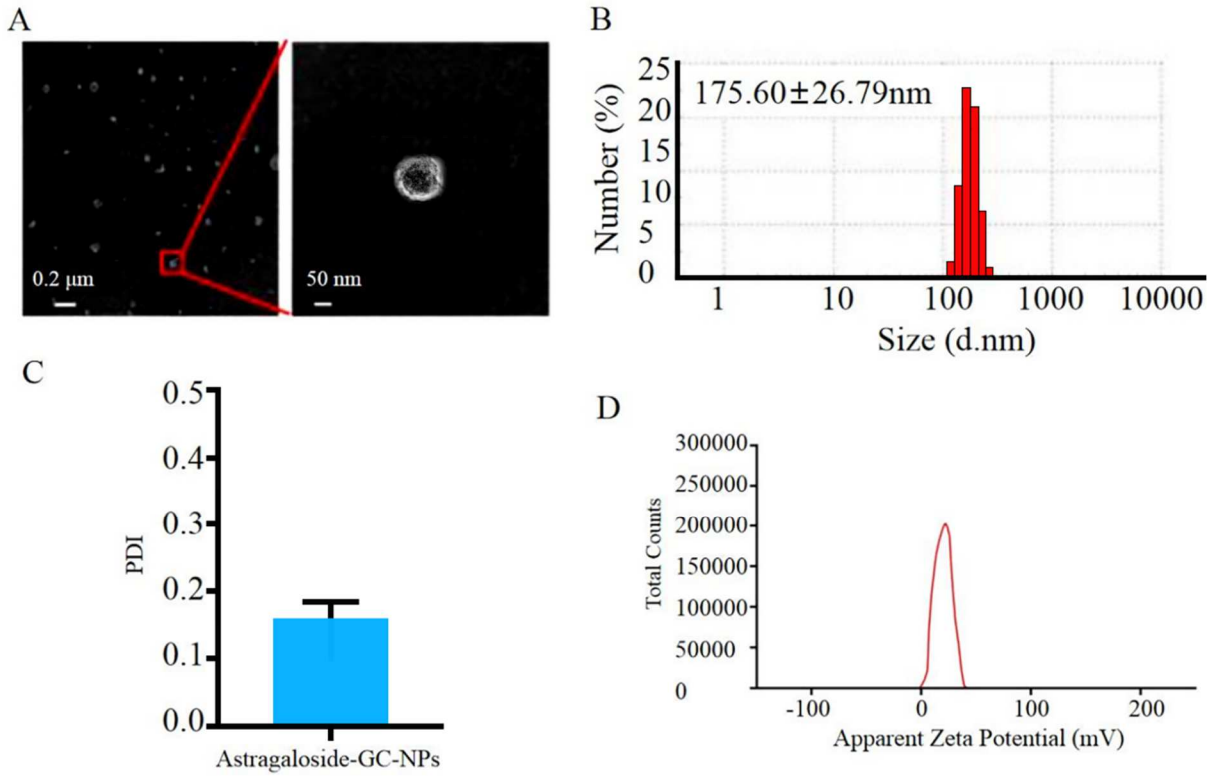

Fig. 3: Electron microscope and potential diagram of Astragaloside-GC-NPs.
(A) Scanning electron microscope image of Astragaloside-GC-NPs; (B) Particle size of Astragaloside-GC-NPs; (C) Measurement of PDI of Astragaloside-GC-NPs by dynamic light scattering method; (D)Potential image of Astragaloside-GC-NPs.

More and more evidence shows the involvement of MAPK/ERK signaling in the behaviors CRC cells and its overexpression and activation can promote the progression of CRC (Liu *et al*., 2024; Li *et al*., 2025b). Motosugi *et al*., (2025) found that Porphyromonas gingivalis (*P.gingivalis*) can invade cells and promote colorectal cancer cells proliferation. In this experiment, it was found highly expressed MAPK/ERK signaling in CRC tumor tissues and after treatment with Astragaloside-GC-NPs, MAPK and ERK phosphorylation was significantly reduced and the MAPK/ERK signaling pathway was inhibited. After injection of miR-200 inhibitor, it can be found that the phosphorylation levels of MAPK and ERK are restored to a high expression state and the MAPK/ERK signaling pathway is activated again. It suggested that miR-200 could regulate the activity of MAPK/ERK signaling pathway. In order to further explore whether Astragaloside-GC-NPs can affect the activity of MAPK/ERK through miR-200 and thus inhibit the development of CRC, we co-injected miR-200 interference fragments and MAPK signaling pathway inhibitor SB202190 into mice to detect CRC Angiogenesis and apoptosis in tumor tissues in mice. This study also found that ALCNPs inhibited p-ERK while simultaneously reducing p-p38 MAPK levels. Notably, rescue experiments using the specific p38 MAPK inhibitor SB202190 confirmed that inhibiting p38 MAPK could partially counteract the phenotypic reversal caused by the loss of miR-200 function. This strongly suggests that p38 MAPK is a key downstream effector molecule of miR-200 within this regulatory axis. Therefore, this study has revealed a core axis by which ALCNPs regulate tumor progression through miR-200: ALCNPs can promote the release of miR-200, thereby inhibiting the p38 MAPK signaling pathway (Badawy *et al*., 2023), thereby inhibiting the formation of blood vessels and ultimately promoting the apoptosis of colon cancer cells (Zheng *et al*., 2022). However, the study has certain limitations. First, as the specific p38 MAPK inhibitor SB202190 was used, the experiments primarily validated the role of the p38 MAPK branch and could not directly prove that the inhibition of ERK1/2 is also a direct result of miR-200 regulation. Second, the inhibition of MAPK/ERK and the reduction in VEGF occurred concurrently and the current data cannot strictly distinguish whether the former is a direct targeting effect of miR-200 or a secondary response following anti-angiogenesis. Future work should employ experiments such as dual-luciferase reporter assays to directly verify whether miR-200 binds to the 3'UTR of upstream molecules in the ERK pathway, such as KRAS or RAF and explore the interaction between p38 MAPK and ERK in this process. This would more precisely delineate the complete downstream signaling network of ALCNPs/miR-200.

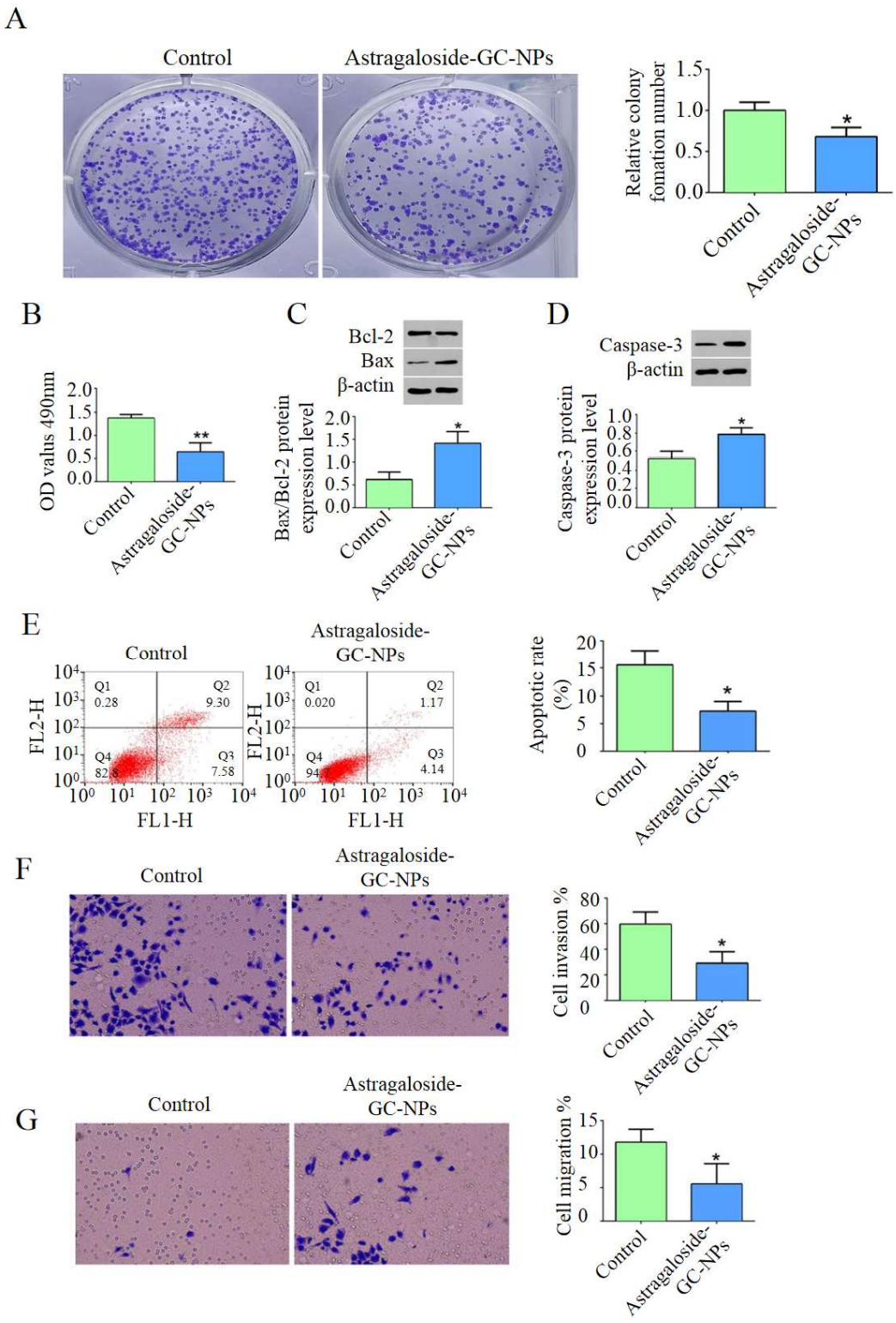

Fig. 4: The effect of Astragaloside-GC-NPs on the biological behavior of CRC cells. ($\bar{x}\pm$s, n=6, two-tailed Student's t-test)

(A) Colony assay to detect the proliferation ability of CRC cells; (B) CCK8 to detect the activity of CRC cells, n=6 complex Wells; (C-D) Western blot to detect the changes of apoptosis-related proteins in CRC cells; (E) Flow cytometry to detect the apoptosis rate; (F-G) Transwell assay for cell invasion and migration, Scale: 100 μm. Compared with Control group, $P<0.05$, $P<0.01$

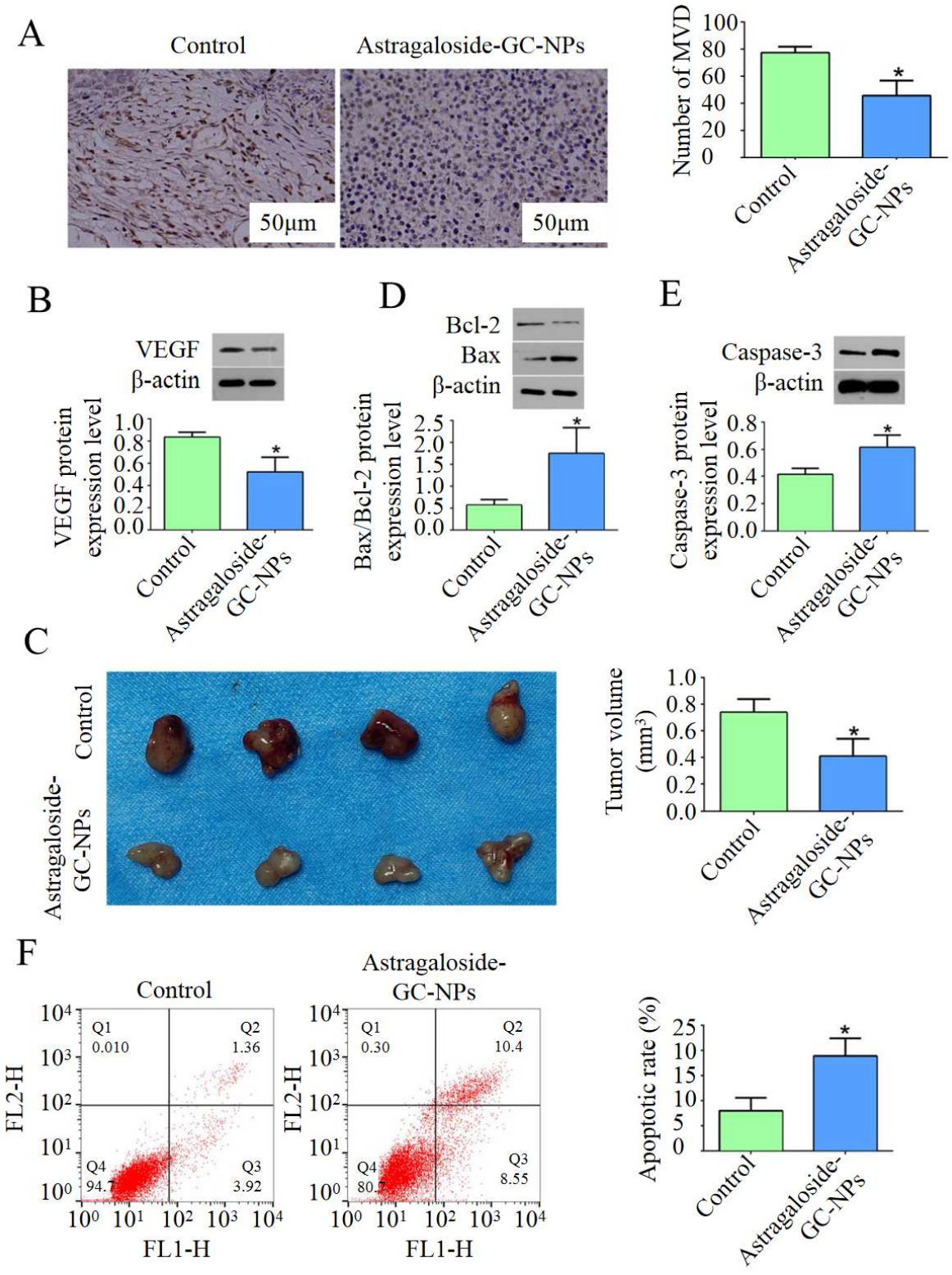

Fig. 5: Effects of Astragaloside-GC-NPs on angiogenesis and tumor tissue apoptosis in CRC mice. ($\bar{x}\pm s$, n=6, two-tailed Student's t-test)

(A) MVD counting to detect the number of Astragaloside-GC-NPs angiogenesis (DAB staining), Scale: 50 μm; (B) Changes in tumor tissue weight; (C) Western blot to detect the expression of VEGF protein; (D-E) Western blot to detect the expression of apoptotic protein; (F) Flow cytometry detection of tumor tissue apoptosis.

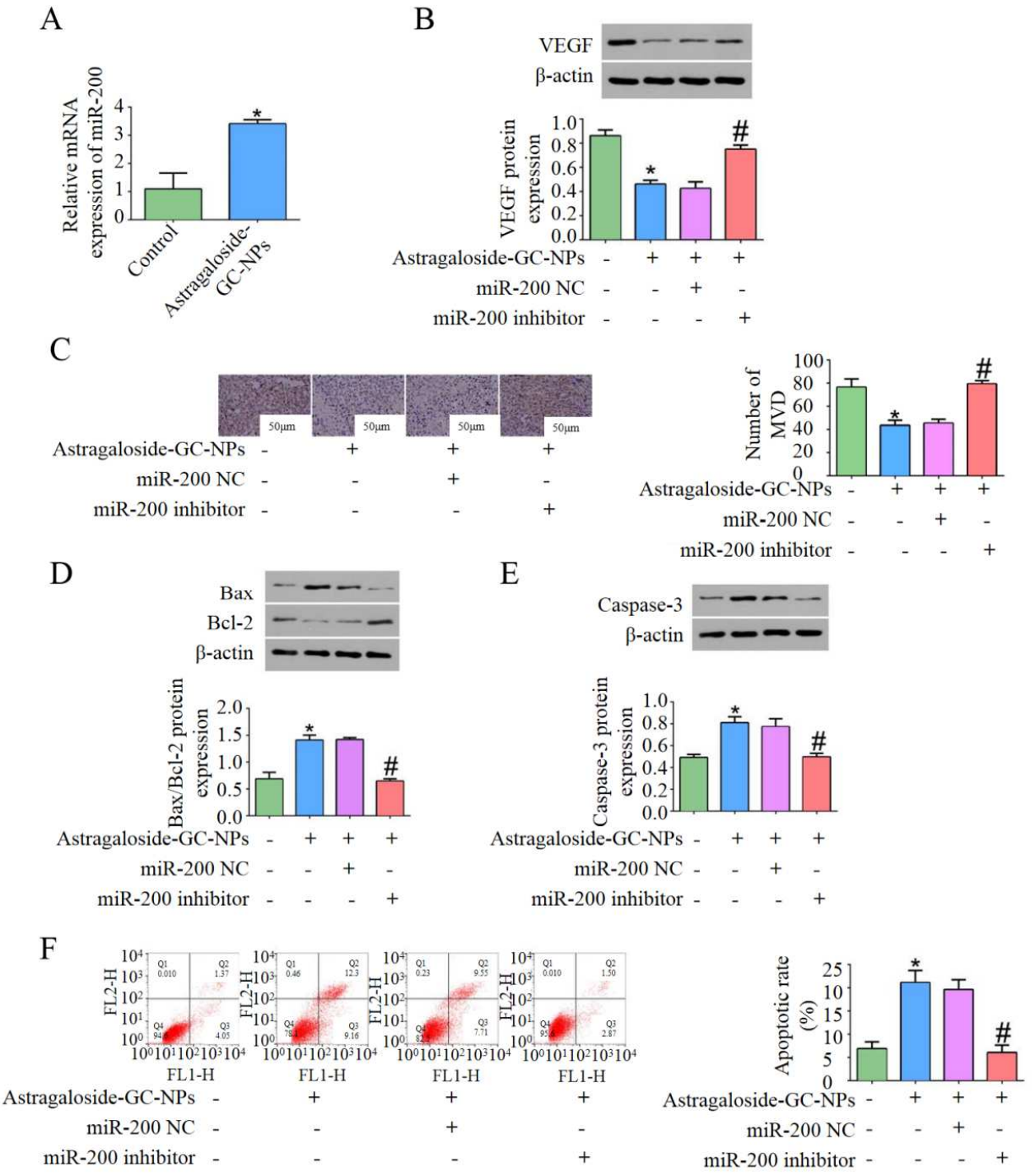

Fig. 6: Effect of Astragaloside-GC-NPs on tumor tissue by regulating miR-200. ($\bar{x}\pm s$, n=6, two-tailed Student's t-test) (A) q-RT PCR to detect the expression of miR-200; (B) Western blot to detect the expression of VEGF protein; (C) MVD count to detect the number of new blood vessels (DAB staining); (D-E) Western blot to detect apoptosis-related proteins (F) Flow cytometry detection of tumor tissue apoptosis. Compared with the Control group, *P<0.05 #P<0.05

Therefore, this study not only reveals the mechanism by which ALCNPs inhibit angiogenesis and promote apoptosis in CRC cells through the regulation of the miR-200/MAPK/ERK axis but also preliminarily demonstrates their therapeutic potential as a novel nano-targeted delivery system. However, the study has several limitations. The experiments were primarily conducted using a mouse subcutaneous xenograft model, which differs from the actual pathological microenvironment in humans.

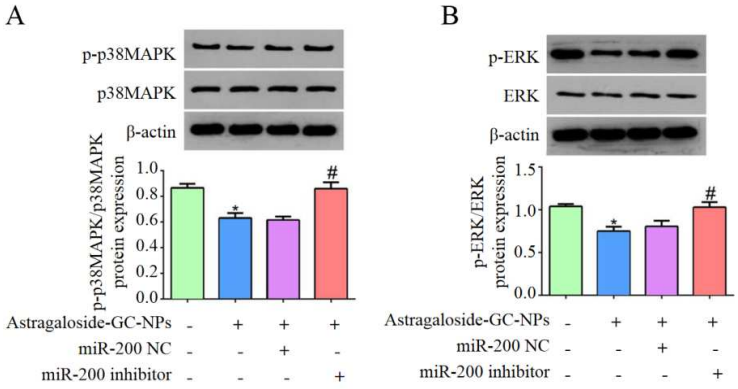

Fig. 7: Effect of Astragaloside-GC-NPs on MAPK/ERK signaling pathway.
($\bar{x} \pm s, n = 6, two - factor$ analysis of variance and Tukey post hoc test) (A-B) Western blot detection of phosphorylation expression levels of p38MAPK and ERK. Compared with Control group, *P<0.05; compared with Astragaloside-GC-NPs+miR-200 NC group, #P<0.05

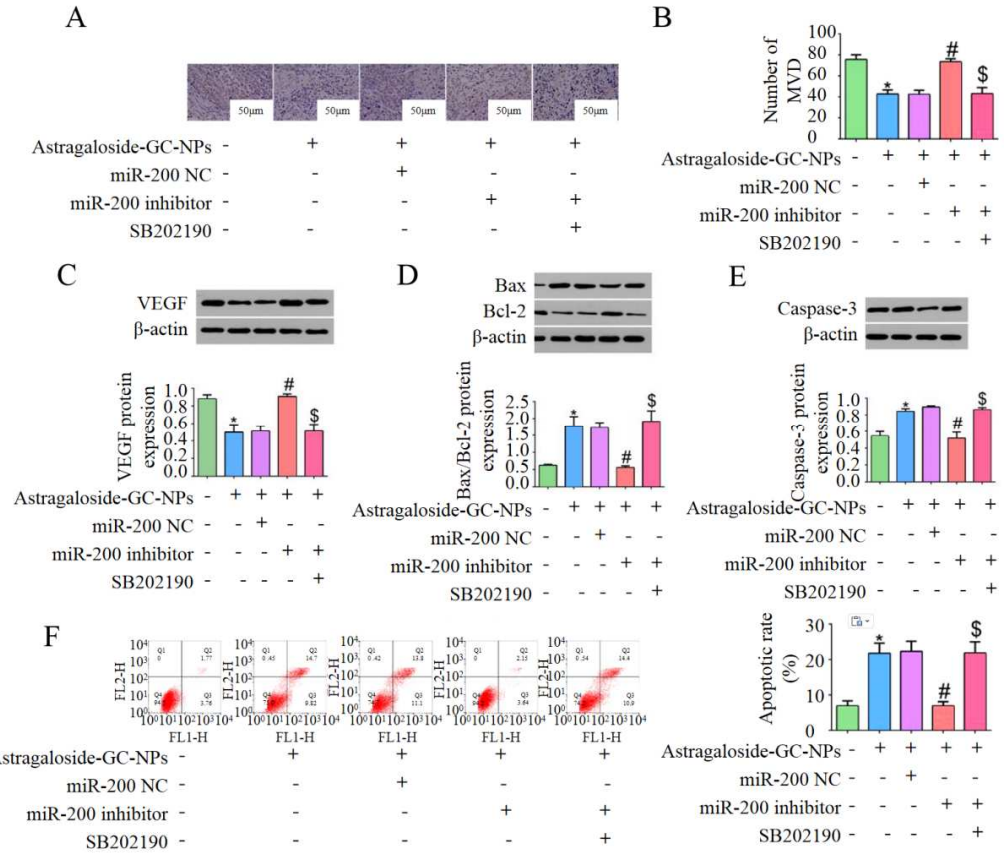

Fig. 8: Effects of overexpression of miR-200 and MAPK inhibitors on apoptosis of CRC tumor tissues.
($\bar{x} \pm s, n = 6, two - factor$ analysis of variance and Tukey post hoc test) (A-B) MVD counting to detect the number of new blood vessels (DAB staining); (C) Western blot to detect the expression of VEGF protein; (D-E) Western blot to detect the expression of apoptosis-related proteins; (F) Flow cytometry to detect the apoptosis of CRC cells Mortality. Compared with Control group, *P<0.05; compared with Astragaloside-GC-NPs+miR-200 NC group, #P<0.05; Astragaloside-GC-NPs+miR-200 inhibitor+SB202190, $P<0.05.

The systemic pharmacokinetics, long-term biosafety and stability during scaled-up production of ALCNPs have not been fully evaluated. Moreover, miR-200, as a therapeutic target, involves complex regulatory mechanisms *in-vivo* and exogenous delivery still faces challenges such as stability, targeting specificity and immunogenicity. Future efforts should focus on validating efficacy in more clinically relevant models, such as orthotopic or patient-derived xenograft (PDX) models and deepening research on formulation optimization, safety assessment and mechanistic exploration to advance the translation of ALCNPs toward clinical application.

CONCLUSION

In summary, this study can prove that Astragaloside-GC-NPs, as a therapeutic drug for CRC, can reduce the formation of neovascularization and slow down the development of CRC mice. Since miR-200 is in a low expression state in tumor tissue, we found that significantly increased miR-200 after treating CRC mice with Astragaloside-GC-NPs. Further studies have confirmed that when Astragaloside-GC-NPs treats the specific mechanism of CRC, miR-200 can inhibit the further development of angiogenesis and cancer in CRC mice by regulating MAPK/ERK signaling. When miR-200 is interfered, the flushing of MAPK/ERK signaling pathway inhibited by Astragaloside-GC-NPs will be activated and when miR-200 is interfered and MAPK signaling is inhibited, the amount of angiogenesis will be increased. While reducing to a certain extent, it increases the apoptosis ability of tumors. This opens up new targeted therapy drugs and research directions for the nano-treatment of CRC, the reduction of angiogenesis in tumor tissue and the development of CRC.

Acknowledgments
There are no acknowledgments.

Authors' contributions
Renhao Chen: Experimental design, data collection Experimental execution, data processing and analysis, manuscript writing;
Bin Wang: Research supervision, Material provision, technical support, manuscript revision and review.
All authors have read and agreed to the final version of the manuscript.

Funding
There was no funding received for this work.

Data availability statement
The datasets generated and/or analyzed during the current study period can be obtained from the corresponding authors upon reasonable request.

Ethical approval
This study was approved by the ethics committee of School of Clinical Medicine, Jiangxi Medical College (JXMC-E-20230309). This study was performed in adherence with the ARRIVE guidelines. See supplementary file for the ARRIVE checklist.

Conflict of interest
The authors declare that this study was conducted in the absence of any commercial or financial relationships that could be construed as a potential conflict of interest. There are no conflicts to declare.

Supplementary data
https://www.pjps.pk/uploads/2026/07/SUP1784550935.pdf

REFERENCES

Badawy MMM, Abdel-Hamid GR and Mohamed HE (2023). Antitumor activity of chitosan-coated iron oxide nanocomposite against hepatocellular carcinoma in animal models. *Biol Trace Elem Res*., **201**(3): 1274-1285.

Chen S, Tu Y, Yuan H, Shi Z, Guo Y, Gong W and Tu S (2022). Regulatory functions of miR-200b-3p in tumor development (Review). *Oncology reports.*, **47**(5): 96.

Cheon I, Lee S, Oh S and Ahn YH (2024). miR-200-mediated inactivation of cancer-associated fibroblasts via targeting of NRP2-VEGFR signaling attenuates lung cancer invasion and metastasis. *Mol Ther Nucleic Acids.*, **35**(2): 102194

Cınar Ayan I, Cetinkaya S, Dursun HG and Suntar I (2021). Bioactive compounds of rheum ribes L. and its anticancerogenic effect via induction of apoptosis and miR-200 family expression in human colorectal cancer cells. *Nutr Cancer*., **73**(7): 1228–1243.

Dai S, Zhuang H, Li Z, Chen Z, Chai Y and Zhou Q (2024). miR-122/NEGR1 axis contributes colorectal cancer liver metastasis by PI3K/AKT pathway and macrophage modulation. *J Transl Med*., **22**(1): 1060.

Dong Y, Zhang N, Zhao S, Chen X, Li F and Tao X (2019). miR-221-3p and miR-15b-5p promote cell proliferation and invasion by targeting Axin2 in liver cancer. *Oncol Lett*, **18**(6): 6491-6500.

Gorecki I and Rak B (2021). The role of microRNAs in epithelial to mesenchymal transition and cancers; Focusing on mir-200 family. *Cancer Treat Res Commun*., **28**: 100385.

Klicka K, Grzywa TM, Mielniczuk A, Klinke A and Włodarski PK (2022). The role of miR-200 family in the regulation of hallmarks of cancer. *Front Oncol*., **12**: 965231.

Li J, Fan S, Li H, Hu Z and Hu Q (2025a). Evaluation of efficacy, safety and underlying mechanism on Traditional Chinese medicine as synergistic agents for cancer immunotherapy: A preclinical systematic review and meta-analysis. *J Ethnopharmacol*., **338**(1): 119035.

Li JQ, Shi YH, Min-Xu Shi CX, Teng-Wang Wang T H, Zuo ZF and Liu XZ (2024). Discovery of astragaloside IV against high glucose-induced apoptosis in retinal ganglion cells: Bioinformatics and in vitro studies. *Gene*., **905**: 148219.

Li Q, Wang Y, Yuan Z, Zhai P, Wang J, Zhang C, Shao Z and Xing C (2025b). YWHAH-driven autophagy via MAPK/ERK signaling enhances CRC cell migration and invasion. *Int J Mol Med*., **56**(6): 228.

Li W, Ke C, Yang C, Li J, Chen Q, Xia Z and Xu J (2023). LncRNA DICER1-AS1 promotes colorectal cancer progression by activating the MAPK/ERK signaling pathway through sponging miR-650. *Cancer Med*., **12**(7): 8351–8366.

Liang Y, Chen B, Liang D, Quan X, Gu R, Meng Z, Gan H, Wu Z, Sun Y, Liu S and Dou G (2023). Pharmacological

effects of astragaloside IV: A review. *Molecules*, **28**(16): 6118.

Liu J, Zhang F, He J, Wang S, Wang L, Li J, Shi W, Han Y, Gao A and Sun Y (2023). Tumor-derived Immunoglobulin-like transcript 4 facilitates angiogenesis of colorectal cancer. *Am J Cancer Res*., **13**(2): 419–435.

Liu W, Tang J, Gao W, Sun J, Liu G and Zhou J (2024). PPP2R1B abolishes colorectal cancer liver metastasis and sensitizes Oxaliplatin by inhibiting MAPK/ERK signaling pathway. *Cancer Cell Int*., **24**(1): 90.

Lu L, Huang JJ, Mo JT, Da X, Li QX, Fan M and Lu HW (2022). Exosomal lncRNA TUG1 from cancer-associated fibroblasts promotes liver cancer cell migration, invasion, and glycolysis by regulating the miR-524-5p/SIX1 axis. *Cell Mol Biol Lett,* **27**(1).

Maomao C, He L, Dianqin S, Siyi H, Xinxin Y, Fan Y, Shaoli Z, Changfa X, Lin L, Ji P and Wanqing C (2022). Current cancer burden in China: Epidemiology, etiology and prevention. *Cancer Biol Med*., **19**(8): 1121–1138.

Morgan E, Arnold M, Gini A, Lorenzoni V, Cabasag C J, Laversanne M, Vignat J, Ferlay J, Murphy N and Bray F (2023). Global burden of colorectal cancer in 2020 and 2040: incidence and mortality estimates from GLOBOCAN. *Gut*., **72**(2): 338–344.

Mortezaee K (2021). Normalization in tumor ecosystem: Opportunities and challenges. *Cell Biol Int*., **45**(10): 2017–2030.

Motosugi S, Takahashi N, Mineo S, Sato K, Tsuzuno T, Aoki-Nonaka Y, Nakajima N, Takahashi K, Sato H, Miyazawa H, Taniguchi K, Terai S and Tabeta K (2025). Enrichment of Porphyromonas gingivalis in colonic mucosa-associated microbiota and its enhanced adhesion to epithelium in colorectal carcinogenesis: Insights from *in-vivo* and clinical studies. *PLoS One*., **20**(3): e0320383.

Pashirzad M, Khorasanian R, Fard MM, Arjmand M H, Langari H, Khazaei M, Soleimanpour S, Rezayi M, Ferns GA, Hassanian SM and Avan A (2021). The therapeutic potential of MAPK/ERK inhibitors in the treatment of colorectal cancer. *Curr cancer drug targets*, **21**(11): 932–943.

Peng Y, Feng H, Wang C, Song Z, Zhang Y, Liu K, Cheng X and Zhao R (2021). The role of E26 transformation-specific variant transcription factor 5 in colorectal cancer cell proliferation and cell cycle progression. *Cell Death Dis*., **12**(5): 427.

Qiu L, Luo W, Chen Y, Guo Z, Quan J, Chi J, Guan Y, Huang Y and Lin Y (2025). The incidence, mortality and survival rate of colorectal cancer in Xiamen, China, from 2011 to 2020. *BMC Public Health*, **25**(1): 176.

Rahman A, Shah M and Shord SS (2024). Dosage optimization: A regulatory perspective for developing oncology drugs. *Clin Pharmacol Ther*., **116**(3): 577–591.

Valenzuela G, Contreras HR, Marcelain K, Burotto M and Gonzalez-Montero J (2025). Understanding microRNA-mediated chemoresistance in colorectal cancer treatment. *Int J Mol Sci*., **26**(3): 1168.

Wang Y, Zhang Z, Cheng Z, Xie W, Qin H and Sheng J (2023). Astragaloside in cancer chemoprevention and therapy. *Chin Med J (Engl)*, **136**(10): 1144–1154.

Xi Y and Xu P (2021). Global colorectal cancer burden in 2020 and projections to 2040. *Transl Oncol*., **14**(10): 101174.

Xia D, Li W, Tang C and Jiang J (2023). Astragaloside IV, as a potential anticancer agent. *Front Pharmacol*., **14**: 1065505.

Xu F, Cui WQ, Wei Y, Cui J, Qiu J, Hu LL, Gong W Y, Dong JC and Liu BJ (2023). Correction: Astragaloside IV inhibits lung cancer progression and metastasis by modulating macrophage polarization through AMPK signaling. *J Exp Clin Cancer Res.R*, **42**(1): 70.

Yang H, He C, Bi Y, Zhu X, Deng D, Ran T and Ji X (2022). Synergistic effect of VEGF and SDF-1α in endothelial progenitor cells and vascular smooth muscle cells. *Front Pharmacol*, **13**: 914347.

Yu Liu X, Ying Mao H, Hong S, Jin CH, Jiang HL and Guan Piao M (2024). Dual-targeting galactose-functionalized hyaluronic acid modified lipid nanoparticles delivering silybin for alleviating alcoholic liver injury. *Int J Pharm*., **666**: 124662.

Zhang XF, Wang T, Wang ZX, Huang KP, Zhang Y W, Wang GL, Zhang HJ, Chen ZH, Wang CY, Zhang JX and Wang H (2021). Hypoxic ucMSC-secreted exosomal miR-125b promotes endothelial cell survival and migration during wound healing by targeting TP53INP1. *Mol Ther Nucleic Acids*, **26**: 347–359.

Zhang Y, Wang M, Zhang X, Jiang Z, Zhang Y, Fu X, Li Y, Cao D, Han J and Tong J (2022). Helicid Improves lipopolysaccharide-induced apoptosis of C6 cells by regulating SH2D5 DNA methylation via the CytC/Caspase9/Caspase3 signaling pathway. *Contrast Media Mol Imaging*, **2022**, 9242827.

Zheng P, Huang Z, Tong D C, Zhou Q, Tian S, Chen B W, Ning D M, Guo Y M, Zhu W H, Long Y, Xiao W, Deng Z, Lei Y C and Tian X F (2022). Frankincense myrrh attenuates hepatocellular carcinoma by regulating tumor blood vessel development through multiple epidermal growth factor receptor-mediated signaling pathways. *World J Gastrointest Oncol.*, **14**(2): 450–477.

Zhong X, He X, Wang Y, Hu Z, Huang H, Zhao S, Wei P and Li D (2022). Warburg effect in colorectal cancer: The emerging roles in tumor microenvironment and therapeutic implications. *J Hematol Oncol*., **15**(1): 160.

Zhou J, Zhou L, Chen ZY, Sun J, Guo XW, Wang HR, Zhang XY, Liu ZR, Liu J, Zhang K and Zhang X (2025). Remineralization and bacterial inhibition of early enamel caries surfaces by carboxymethyl chitosan lysozyme nanogels loaded with antibacterial drugs. *J Dent.*, **152**: 105489.